Transport Mechanisms of Gases in Annealed Linear Low Density Polyethylene Films

ARTICLE *in* MACROMOLECULES · SEPTEMBER 1998

Impact Factor: 5.8 · DOI: 10.1021/ma971600u

Transport Mechanisms of Gases in Annealed Linear Low Density Polyethylene Films

V. Compañ,[†] M. López-Lidón,[†] A. Andrio,[†] and E. Riande*[,‡]

Departamento de Física Aplicada, Universidad Jaume I, Castellón, Spain, and Instituto de Ciencia y Tecnología de Polímeros (CSIC), 28006 Madrid, Spain

Received October 30, 1997; Revised Manuscript Received June 17, 1998

ABSTRACT: The effect of the pressure difference on the permeability of carbon dioxide, oxygen, and nitrogen through annealed LLDPE films is studied. The isotherms showing the dependence of the permeability coefficient on the pressure of the upstream chamber, p_o, exhibit an anomalous decrease in the low-pressure region whose location is shifted to lower values of p_o as the temperature of the isotherms decreases. The diffusion coefficient increases with p_o, the increase being larger the higher is the temperature. The curves showing the dependence of the solubility coefficient on the pressure of the upstream chamber exhibits the same pattern as that of the permeability coefficient. The strong dependence of the diffusive characteristics of gases on p_o in the low-pressure region was interpreted in terms of the dual mode theory. The values of the apparent diffusion coefficients for the molecules in the dissolved and the trapped modes are estimated. In the same way, the Henry's law solubility coefficient, k_D, and the Langmuir sorption capacity, C'_H, are obtained. The values of k_D and C'_H for different gases are somewhat lower than those reported for glassy membranes. A detailed study on the effect of p_o on the activation energies associated with both the permeability and the diffusion coefficients is reported.

Introduction

Because of their good mechanical properties, especially high tear strength, toughness, and good processability characteristics, coextruded films prepared from linear low-density polyethylene (LLDPE) present a wide variety of uses in the packaging industry.[1] The good mechanical properties of the films arise from the copolymeric nature of LLDPE that makes possible the preparation of films that combine a relatively low crystallinity and a moderate orientation. Since these films are mainly used in food packaging, the study of the diffusive characteristics of gases through them, specially oxygen, nitrogen and carbon dioxide, is of a great importance.

The permeation of gases in LLDPE semicrystalline films is a rather complex process.[2−6] Gas permeation through the amorphous phase of the films is a simple process, similar to that occurring through a liquid, and it is expected that the changes in the permeation characteristics with temperature obey Arrhenius behavior. However, crystalline entities in the semicrystalline films act as impermeable barriers to gases, forcing the penetrants to travel a longer path in the crystalline−amorphous interface than in the amorphous region, thus decreasing the diffusion coefficient.[3] Moreover, as a consequence of the presumable changes in the crystalline−amorphous interface with temperature, the transport of gases in LLDPE films may not be a simple thermal-activated process.

Earlier studies have shown that annealing causes a significant increase in the permeability coefficients of gases in coextruded LLDPE films without changing their overall degree of crystallinity.[7,8] On the other hand, the fact that the apparent diffusion coefficient only slightly decreases with annealing suggests that the most important consequence of this thermal process is a strong increase of the solubility of gases in the films. It would be expected, however, that annealing performed at relatively high temperatures (∼80 °C) would change the crystalline−amorphous interface in two opposing ways: favoring crystallites thickening, and increasing the transition order → disorder in the oriented molecules close to the crystalline−amorphous interface. In view of this, the increase of the apparent solubility coefficients by effect of annealing could be due either to a significant increase in the amorphous rubbery region at the expense of both the oriented regions and the melting of the low size crystalline entities, or to the formation of molecular packing defects in the crystals and/or the crystalline−amorphous interface that could accommodate individual site molecules without disturbing the natural dissolution process of the gas in the amorphous region.[8] The first cause seems unlikely because a significant change in the overall crystallinity of the films is not detected. Therefore the increase in solubility could be attributed to adsorption processes taking place in defects in the crystals and/or in cavities formed in the crystalline−amorphous interfaces. In this case, adsorption processes would play an important role in the gas transport. If this assumption is true, the dual mode model that gives a good account of gas transport in glassy membranes[9,10] would also describe the gas transport in annealed semicrystalline films. According to the model, diffusion would occur by jumps of dissolved molecules in the amorphous region (first mode) and partial mobility of trapped molecules in the cavities (second mode). To test the reliability of this assumption, attention was paid in this work to the study of the permeability of annealed coextruded LLDPE films as a function of the pressure gradient. The results were further interpreted by assuming that Langmiur gas adsorption plays an important role in the solubility characteristics of the films. Attempts were also made to investigate how the combination of pres-

[†] Universidad Jaume I.
[‡] Instituto de Ciencia y Technología de Polímeros.

S0024-9297(97)01600-8 CCC: $15.00
Published on Web 09/15/1998

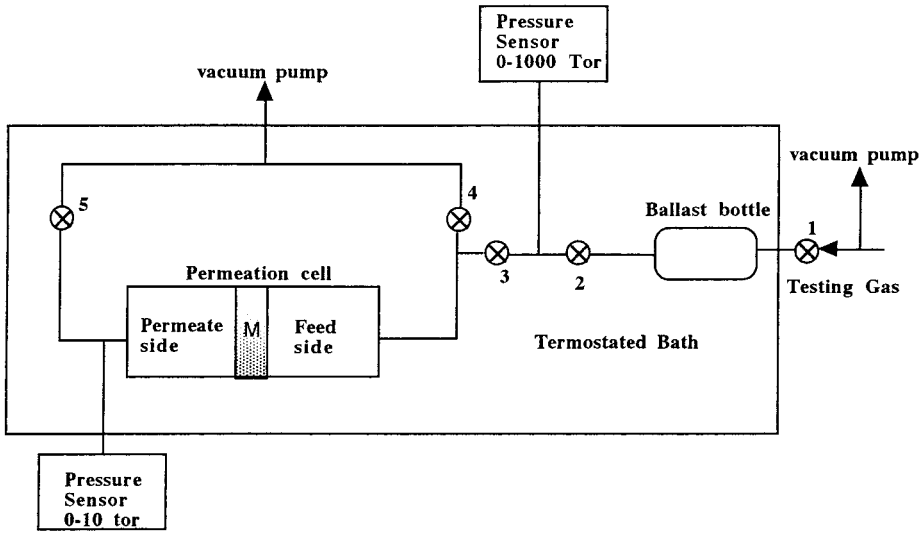

Figure 1. Scheme of the experimental device used in the permeation measurements.

sure and temperature may affect the gas transport and the permselectivity of the coextruded LLDPE films.

Experimental Section

LLDPE films were prepared by coextrusion of 1-octene-*co*-ethylene copolymers of roughly 8% mol content of 1-octene. The films, a gift from Dario Manuli (Italy), were made of three layers, C (15 wt %, $t = 3.5$ μm), A (70 wt %, $t = 16$ μm), and B (15 wt %, $t = 3.5$ μm), where t refers to the thickness of the layers. The C and A layers are Dowlex 2247 ($\rho = 0.917$ g cm^{-3}) while the B layer is Dowlex 2291 ($\rho = 0.912$ g cm^{-3}). The films were processed with three extruders C, A, and B at speeds of 88, 29, and 88 rpm, respectively. Details of the processing conditions are given elsewhere.[1]

The thermogram of the films, determined with a DSC-4 calorimeter at a heating rate of 10 °C min^{-1}, exhibits a blurred melting peak in the vicinity of 38 °C, which presumably corresponds to the melting of low crystalline size entities, followed by a wide melting endotherm extending from 90 °C up to 125 °C with the peak maximum located at 123°. The degree of crystallinity determined from the endotherms amounted to 0.28. The films used in the permeation measurements were annealed at 80 °C for 24 h. The thermograms of these films showed nearly the same pattern that the nonannealed ones, although the small endotherm peak appearing at 38 °C in the latter films was not detected. The degree of crystallinity of the annealed films was 0.30.

Permeation measurements of N_2, O_2, and CO_2 through the annealed films were carried out in the experimental device shown in Figure 1. Keeping the valves 3, 4, and 5 open and valve 2 closed, high vacuum ($\sim 10^{-4}$ mmHg) was made for 24 h in the upstream and downstream chambers separated by the films. Valves 4 and 5 were then closed, valve 2 was opened, and the testing gas, kept in a ballast bottle placed inside a thermostated bath at a pressure close to that used in the experiment, suddenly flowed into the high-pressure chamber. Taking as zero the time at which valve 2 was open, the evolution of the pressure in the downstream chamber with time was monitored with a transducer pressure sensor (0−10 mmHg). Before each series of measurements, the system was vacuum calibrated by measuring the inlet of air into the downstream chamber.

Results

The plots showing the time dependence of the pressure in the downstream chamber present, as usual, a transient state at short times and steady-state transport conditions at long times. The intercept of the extrapolated steady-state part of the curve with the time axis gives the time-lag θ which is related to the apparent diffusion coefficient, D, by the following expression suggested by Barrer:[11]

$$D = L^2/(6\theta) \tag{1}$$

where L is the thickness of the films. The permeability coefficient P can be obtained from the slope of the steady-state part of the curves by means of the equation

$$P = \frac{273}{76}\left(\frac{VL}{ATp_o}\right)\left(\frac{dp(t)}{dt}\right) \tag{2}$$

where V is the volume of the low-pressure chamber, A is the effective area of the film, p_o is the pressure, in centimeters of Hg, of the penetrant gas in the upstream chamber, $dp(t)/dt$ is the slope of the steady-state part of the curve that shows the time dependence of the pressure of the gas in the downstream chamber, and T is the absolute temperature. The diffusion coefficient is usually given in centimeters squared per second, while P is expressed in barrers (1 barrer = 10^{-10}(cm^3-(STP)cm)/(cm^2 s cmHg)).

Owing to the relatively low values of θ obtained for the very thin semicrystalline rubbery films used in this study, significant errors can be involved in the determination of the diffusion coefficient by the time-lag method. To increase the value of this quantity and thus diminish the uncertainty of the value of D, transport measurements were performed in membranes made up of three films firmly stuck together with a rolling cylinder at room temperature. However, heterogeneities in the interfaces arising from gas vowels formed between two consecutive layers could alter the values of the time lag in the membrane. This possibility was tested by measuring the time lags for the permeation of CO_2, N_2, and O_2 in membranes made up of 1, 2, 3, 4, and 5 layers. The results obtained, shown in Figure 2, indicate that the time lag of the gases used in this study scales with the square of the number of layers of the membrane, as eq 1 suggests for homogeneous membranes. Consequently boundary effects are not impor-

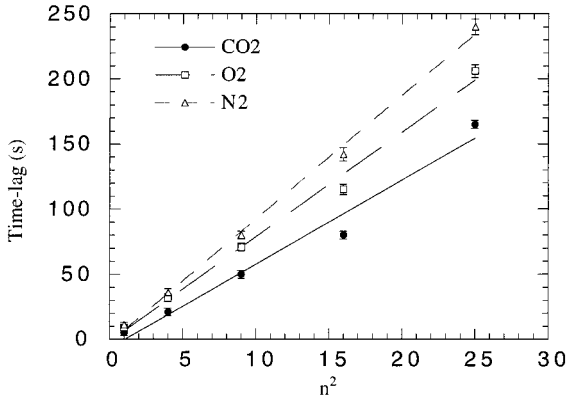

Figure 2. Dependence of time lags of CO_2, O_2 and N_2, at 25 °C, on the square number of layers, n^2, of LLDPE membranes.

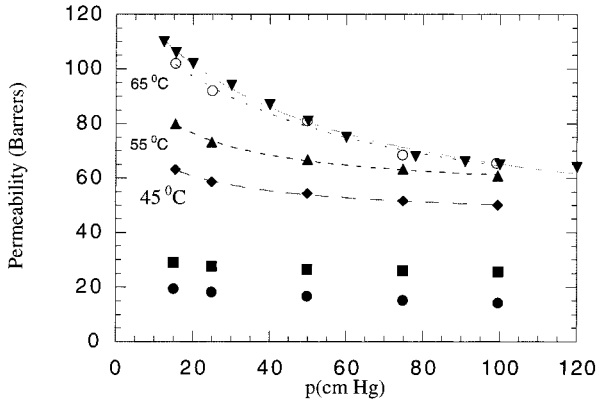

Figure 3. Variation of the permeability coefficient of carbon dioxide with the pressure of the upstream chamber at several temperatures: (●) 25, (■) 35, (◆) 45, and (○) 55 °C. The curve at 65 °C includes two sets of experiments with 5 (○) and 11 points (▼), respectively.

tant in the study of the gas transport through the multilayer LLDPE membranes used in this work.

The relative error, Δ, involved in the determination of the diffusion coefficient by the time-lag method was obtained by the following expression

$$\Delta = 100\left[\left|\frac{L\epsilon(L)}{3\theta}\right| + \left|\frac{L^2\epsilon(\theta)}{6\theta^2}\right|\right]/D \qquad (3)$$

where $\epsilon(L)$ and $\epsilon(\theta)$ are, respectively, the errors involved in the evaluation of the thickness of the membranes and the time lag, respectively. It should be pointed out that even in the most unfavorable case (highest temperature), the error estimated in the determination of the apparent diffusion coefficient in membranes made up of three layers was lower than 10%.

Values of the permeability coefficient for CO_2, N_2, and O_2, at different temperatures, are plotted as a function of the pressure of the upstream chamber in Figures 3, 4, and 5, respectively. All the curves exhibit the same pattern, in the sense that the permeability coefficient decreases with increasing pressure. An important characteristic of the isotherms obtained at temperatures above 45 °C is that the values of the permeability coefficient undergo an anomalous increase or upturn with decreasing p_o in the low-pressure region. Moreover, the results suggest that the region in which this increase occurs is shifted to lower pressures as the temperature decreases. It is worth noting that the upturn in the curves P against p_o is not detected at

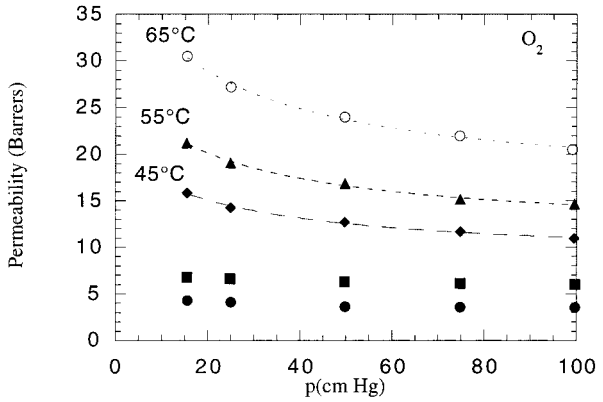

Figure 4. Dependence of the permeability coefficient of oxygen on the pressure of the upstream chamber at several temperatures: (●) 25, (■) 35, (◆) 45, (▲) 55, and (○) 65 °C.

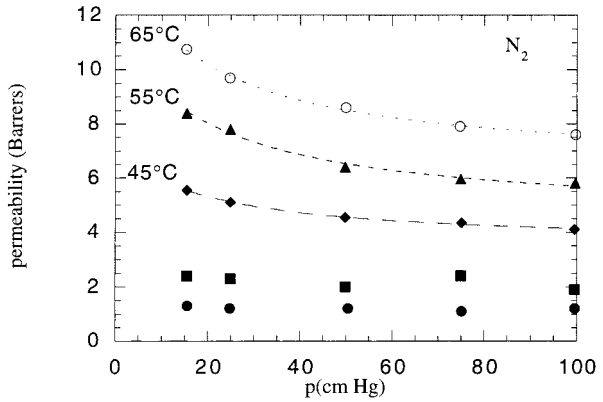

Figure 5. Isotherms showing the variation of the permeability coefficient of nitrogen with the pressure of the upstream chamber: (●) 25, (■) 35, (◆) 45, (▲) 55, and (○) 65 °C.

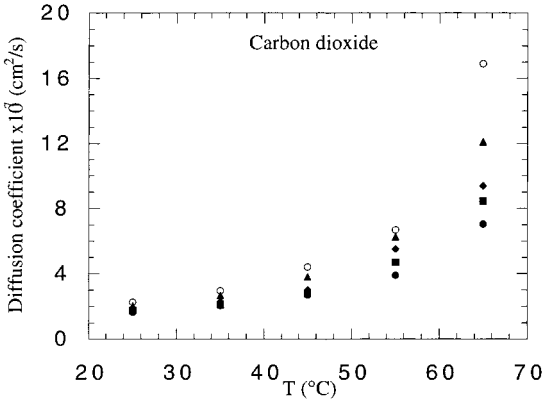

Figure 6. Variation of the diffusion coefficient of carbon dioxide with temperature for different values of the pressure of the upstream chamber: (●) ≅15.5, (■) ≅24.9, (◆) ≅49.8, (▲) ≅74.8, and (○) ≅95.5 cmHg.

temperatures below 35 °C; the upturn in the low-temperature isotherms could be shifted to pressures below 100 mmHg, the lowest value of the pressure of the upstream chamber used in this study. As usual,[12] the permeability coefficient follows the trend $P(CO_2) > P(O_2) > P(N_2)$, independently on the pressure used in the upstream chamber.

Results for the apparent diffusion coefficients of CO_2, O_2, and N_2, at different temperatures and pressures, are given in Figures 6, 7, and 8, respectively. It can be seen that the values of D increase with both the temperature and the pressure of the upstream chamber. Moreover,

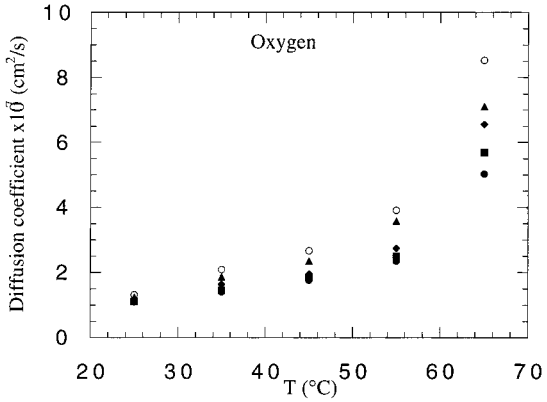

Figure 7. Isobars showing the temperature dependence of the diffusion coefficient of oxygen on temperature: (●) ≅15.5, (■) ≅24.9, (◆) ≅49.8, (▲) ≅74.8, and (○) ≅95.5 cmHg.

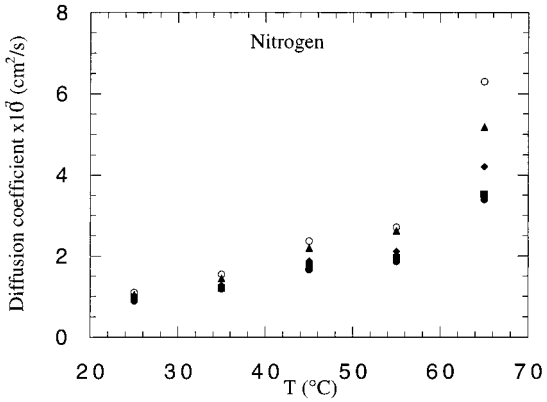

Figure 8. Dependence of the diffusion coefficient of nitrogen on temperature for different pressures of the upstream chamber: (●) ≅15.5, (■) ≅24.9, (◆) ≅49.8, (▲) ≅74.8, and (○) ≅95.5 cmHg.

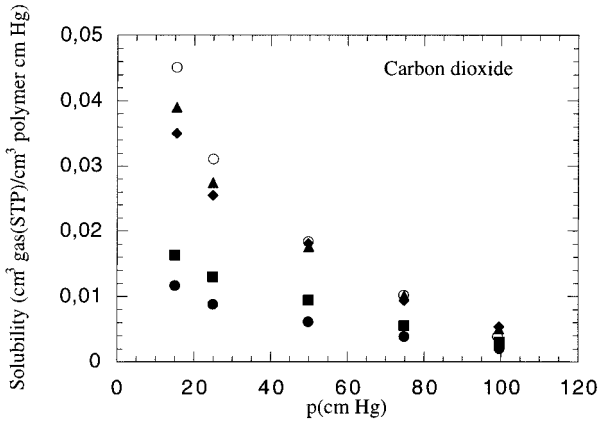

Figure 9. Isotherms showing the variation of the solubility coefficient of carbon dioxide with the pressure of the upstream chamber: (●) 25, (■) 35, (◆) 45, (▲) 55, and (○) 65 °C.

the diffusion coefficients follow the same trend as the permeability coefficients, that is, $D(CO_2) > D(O_2) > D(N_2)$.

The apparent solubility coefficient, S, can be written as

$$S = P/D \tag{4}$$

the units of S being cm^3 gas/cm^3 cmHg. The values of S at different temperatures are plotted as a function of the pressure of the upstream chamber in Figures 9, 10, and 11 for CO_2, O_2, and N_2, respectively. An inspection

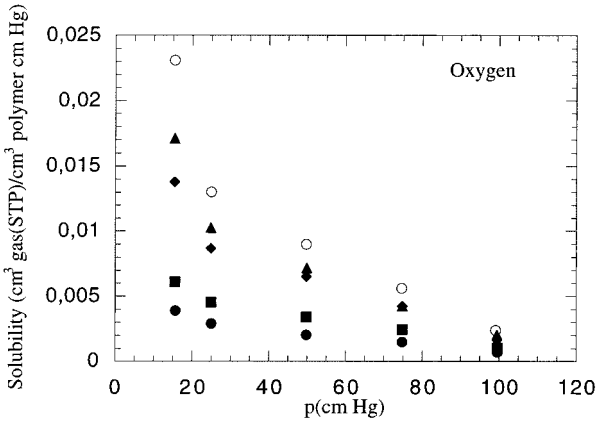

Figure 10. Variation of the solubility coefficient of oxygen with the pressure of the upstream chamber at several temperatures: (●) 25, (■) 35, (◆) 45, (▲) 55, and (○) 65 °C.

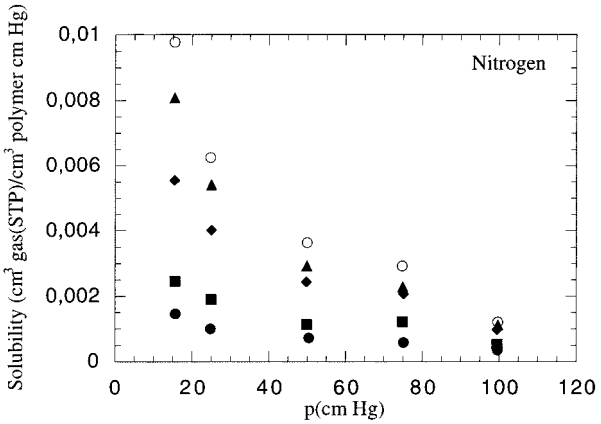

Figure 11. Dependence of the solubility coefficient of nitrogen on the pressure of the upstream chamber at several temperatures: (●) 25, (■) 35, (◆) 45, (▲) 55, and (○) 65 °C.

of the curves reveals that the solubility coefficient increases as p_o decreases. In general the curves exhibit the same pattern that those corresponding to the permeability coefficient.

Discussion

The anomalous dependence of the transport properties on the upstream pressure suggests that the apparent solubility of the gases in coextruded LLDPE films could be the result of Henry's solution in the rubbery region and trapping of gas in defects occurring in the crystals and/or the crystalline−amorphous interface. Accordingly, two modes of transport would be responsible for the permeation of the gases through the films. The flow of gas through a membrane governed by the dual mode is described by[13]

$$J = -D_D \nabla C - D_H \nabla C_H \tag{5}$$

where D_D and D_H are, respectively, the apparent diffusion coefficients for the permeant molecules in the dissolved and the trapped modes. This equation is only valid if coupling between the two modes is absent, at first sight an unlikely assumption. However, consideration of coupling between the two modes in the development of flow transport equations leads to complex relationships involving a substantial unknown number of parameters that inhibit their application.[14] As a consequence, the experimental values of the permeability coefficient were interpreted, as usual, in

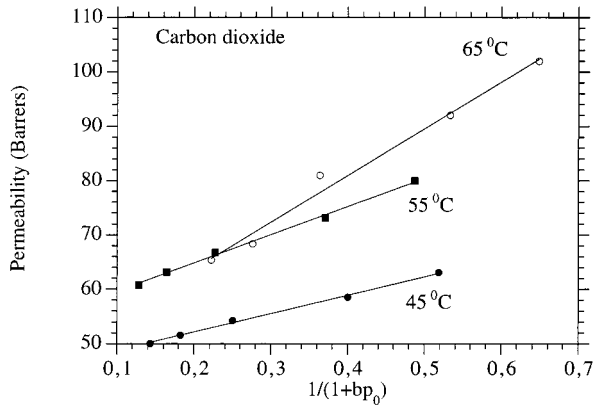

Figure 12. Illustrative plots showing the fitting of the values of permeability coefficient of CO_2, at 45, 55, and 65 °C, to eq 6.

Table 1. Contributions of the First and Second Modes to the Permeability Coefficients of CO_2, O_2, and N_2 through Coextruded LLDPE Membranes

gas	T, °C	$10^{10} \times k_D D_D$[a]	$10^{10} \times C'_H D_H$[a]	b, (cm Hg)$^{-1}$
CO_2	45	45.4 ± 1.3	600 ± 150	0.060 ± 0.025
	55	54.5 ± 1.8	800 ± 200	0.068 ± 0.025
	65	35 ± 17	4500 ± 3000	0.020 ± 0.017
	65[b]	36 ± 5	4000 ± 900	0.023 ± 0.005
O_2	45	8.8 ± 0.8	300 ± 100	0.040 ± 0.020
	55	11.5 ± 0.9	400 ± 100	0.043 ± 0.018
	65	16.3 ± 1.5	600 ± 200	0.042 ± 0.021
N_2	45	3.6 ± 0.2	70 ± 20	0.050 ± 0.025
	55	4.5 ± 0.6	140 ± 80	0.05 ± 0.04
	65	6.4 ± 0.3	150 ± 30	0.056 ± 0.019

[a] $k_D D_D$ and $C'_H D_H$ are given in barrers (1 barrer = 10^{-10}(cm^3(STP) cm)/(cm^2 s cmHg)). [b] These results were obtained with 11 points in the pressure dependence of the permeability coefficient.

terms of the following relationship[13]

$$P = k_D D_D + D_H \frac{C'_H b}{1 + bp_o} \qquad (6)$$

where k_D is the Henry's law solubility coefficient, C'_H is the Langmuir sorption capacity, D_D and D_H are the diffusion coefficients for Henry and Langmuir modes, respectively, and b is an affinity parameter characterizing the ratio of the rate constants for sorption and desorption. Values of P were plotted against $1/(1 + bp_0)$ using different values of b; the right value of b was taken as that one that best fits the plot to a straight line. Illustrative plots of this kind are given in Figure 12. The values of $k_D D_D$ and $D_H C'_H b$ were determined, respectively, from the intercepts and slopes of the straight lines obtained. The results for b at different temperatures are given in the last column of Table 1. The contribution of the first mode, $k_D D_D$, to the permeability coefficient undergoes at each temperature a moderate increase from N_2 to O_2, and a sharp increase from O_2 to CO_2. The same occurs with the term $C'_H D_H$ of the Langmuir mode while the value of b though remains nearly constant in the interval of temperature investigated seems to increase with the size of the diameter of the penetrant molecule.

The apparent values of k_D and C'_H can be estimated from the dependence of the apparent solubility coefficient on p_o given by

$$S = k_D + \frac{bC'_H}{1 + bp_o} \qquad (7)$$

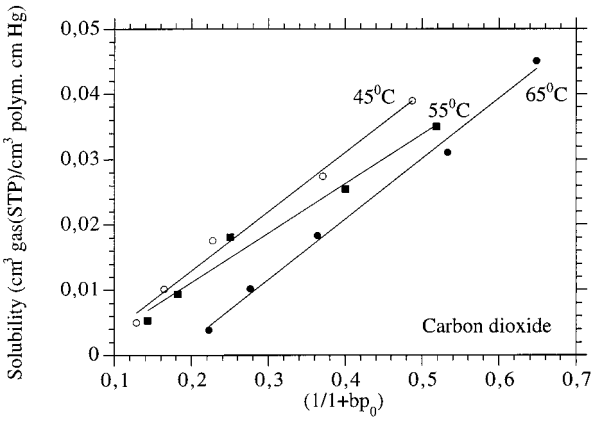

Figure 13. Illustrative plots showing the fitting of the values of the solubility coefficient of CO_2, at 45, 55 and 65 °C, to eq 6.

Table 2. Values of the Individual Parameters Associated with the First and Second Modes of Transport of CO_2, O_2, and N_2 through Coextruded LLDPE Membranes

gas	T, °C	$10^3 \times k_D$[a]	C'_H[a]	$10^7 \times D_D$[a]	$10^7 \times D_H$[a]
CO_2	45	7.3 ± 1.4	0.53 ± 0.2	6.2 ± 1.2	1.1 ± 0.7
	55	5.0 ± 1.1	0.45 ± 0.2	10.9 ± 2.4	1.8 ± 1.2
	65	0.9 ± 0.5	1.14 ± 0.3	41 ± 4	3.5 ± 1.7
O_2	45	2.1 ± 0.2	0.28 ± 0.16	4.2 ± 0.6	1.1 ± 1.0
	55	1.5 ± 0.2	0.30 ± 0.15	7.7 ± 1.4	1.3 ± 1.0
	65	0.9 ± 0.2	0.20 ± 0.11	18 ± 5	3.0 ± 2.5
N_2	45	0.9 ± 0.1	0.12 ± 0.06	4.0 ± 0.7	0.6 ± 0.5
	55	1.0 ± 0.2	0.13 ± 0.06	4.5 ± 1.5	1.1 ± 1.1
	65	0.53 ± 0.14	0.09 ± 0.03	12 ± 4	1.7 ± 0.8

[a] The units of k_D and C'_H are cm^3(STP)/(cm^3 cmHg) and cm^3(STP)/cm^3, respectively, while the unit of D_D and D_H is cm^2 s^{-1}.

Table 3. Henry and Lagmuir Parameters for CO_2 in Glassy Membranes (Amorphous Bisphenol A Polycarbonate (PC), Semicrystalline Poly(2,2,4,4-tetramethyl cyclobutane carbonate) (TMCBPC), and Amorphous Tetramethylbisphenol A Polycarbonate (TMBPPC)[10]) and Coextruded LLDPE Membranes

membrane	T, °C	$10^3 \times k_D$[a]	C'_H[a]	$10^3 \times b$ (cm^{-1})
PC	35	8.9	18.8	3.4
TMCBPC	35	15.7	27.6	5.7
TMBPPC	35	13.3	7.9	3.7
LLDPE	45	7.3	0.53	60

[a] The units of k_D and C'_H are cm^3(STP)/(cm^3 cmHg) and cm^3(STP)/cm^3.

Values of S were plotted against $1/(1 + bp_o)$, using for b the results of Table 1. Illustrative plots are shown in Figure 13. From the slopes and intercepts of these plots, the values of C'_H and k_D shown in the second and third columns of Table 2, respectively, were obtained. In Table 3, and for comparative purposes, the values at 35 °C of k_D, C'_H and b for CO_2 are also shown for membranes prepared from amorphous bisphenol A polycarbonate (PC), semicrystalline poly(2,2,4,4-tetramethyl cyclobutane carbonate) (TMCBPC) and amorphous tetramethylbisphenol A polycarbonate (TMBPPC).[10] All of these membranes have high glass transition temperatures; gas solution in these membranes is viewed as a process involving absorption in the homogeneous part of the matrix, and adsorption in microcavities, responsible for the excess of volume in the glassy state, dispersed in a continuous matrix. In general, the values of k_D and C'_H reported for these glassy membranes are larger than those obtained for coextruded LLDPE

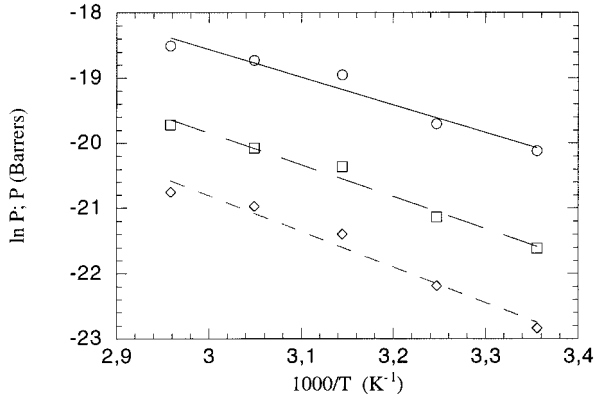

Figure 14. Arrhenius plot of the permeability coefficient of carbon dioxide at 25 cmHg.

membranes. However, the results for b in the latter membranes are significantly larger than those corresponding to the former ones. It is worth noting that the values of k_D for CO_2 in LLDPE membranes are lower than those corresponding to the glassy membranes even if they are related to the amorphous phase. In this case, Henry's constant for LLDPE membranes has a value of 9.1×10^{-3} cm^3 (STP)/(cm^3(amorphous phase) cm Hg) nearly equal to that corresponding to amorphous PC membranes but significantly lower than the values of this quantity for TMCBPC and TMBPPC. This behavior may be due to the fact that attractive interactions are more favored between the CO_2 molecules and the polar chains (PC, TMCBP, and TMBPPC) than between CO_2 and the nonpolar LLDPE chains. On the other hand, the adsorption/desorption rate for CO_2 in LLDPE membranes is significantly larger than that corresponding to this gas in the glassy membranes. To check the reliability of the values of b, this quantity was also obtained from a experimental set in which 11 different pressures were used in the high-pressure chamber. The pertinent results for CO_2 at 65 °C are shown in the fourth row of Table 1. The value of b obtained from these results amounts to 0.023 ± 0.005, very close to that obtained from the set of experiments carried out with only five experimental data.

The results for k_D and C'_H in combination with those obtained for $k_D D_D$ and $C'_H D_H$ allow the determination of D_D and D_H. The values of the diffusion coefficients for the first and second modes, also shown in Table 2, suggest that $D_H/D_D < 1$, in concordance with earlier results indicating that the ratio usually falls into the range 0.04−0.6.[13] Although the temperature dependence of both D_D and D_H seems to follow Arrhenius behavior there are few results to obtain quantitative conclusions regarding the activation energy of the two diffusive modes.

Overall activation energies of the permeation process were obtained by plotting the natural logarithm of the permeability coefficient against the reciprocal of the temperature at different pressures. Illustrative plots of this kind, shown in Figure 14, indicate that despite the complexity of the transport process the results obey fairly well Arrhenius behavior. The values of the activation energy E_P, associated with the gas permeation, are summarized for different values of the pressure of the upstream chamber in Figure 15. As expected, $E_P(N_2) > E_P(O_2) > E_P(CO_2)$, independently on the value of p_o. On the other hand, it is worth noting that for each gas E_P decreases as p_o increases. The

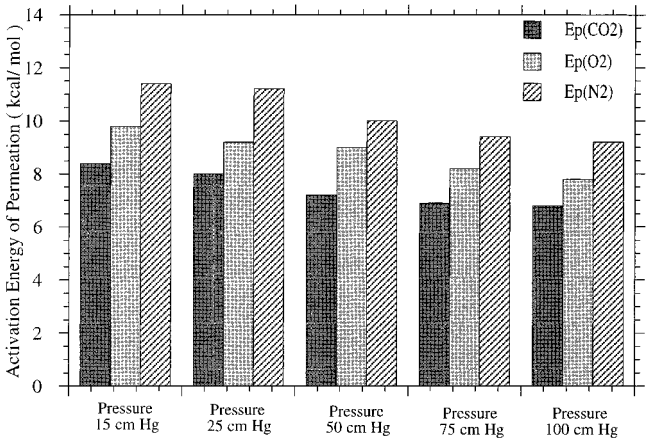

Figure 15. Influence of the pressure of the upstream chamber on the activation energies associated with the permeability coefficients of CO_2, O_2, and N_2.

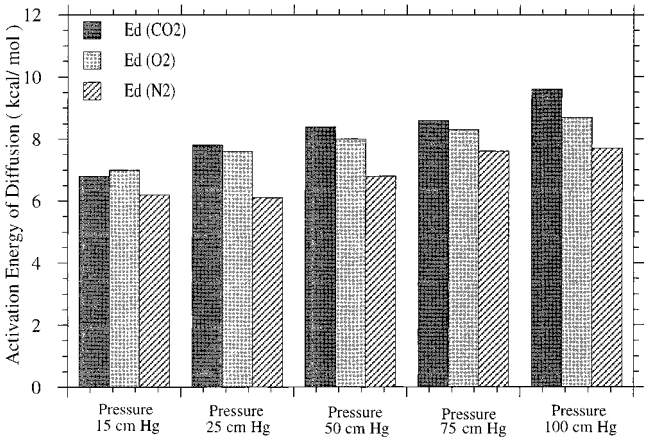

Figure 16. Influence of the pressure of the upstream chamber on the activation energies associated with the diffusion coefficients of CO_2, O_2, and N_2.

temperature dependence of the apparent diffusion coefficient for different gases was also interpreted in terms of the Arrhenius equation. In general the results for the apparent diffusion coefficient fit fairly well to this equation, as the fact that the correlation factor for Arrhenius plots is larger than 0.90 suggests. Values of the activation energies at different pressures are shown in Figure 16 where it can be seen that $E_D(N_2) < E_D(O_2) < E_D(CO_2)$ for each value of p_o. Moreover, the values of the activation energy increase as the pressure goes up. Because $E_S = E_P - E_D$, the inequality $E_S(N_2) > E_S(O_2) > E_S(CO_2)$ will hold for the activation energy associated with the apparent solubility coefficient.

The gas separation factor of a membrane toward gas A relative to gas B is usually expressed by the permselectivity factor α(A/B) given by

$$\alpha(A/B) = [P(A)]/[P(B)] \qquad (8)$$

Illustrative plots showing the temperature dependence $\alpha(CO_2/N_2)$ and $\alpha(CO_2/O_2)$ at $p_o = 25$ cmHg are shown in Figure 17. It can be seen that the values of these quantities which at 25 °C are 16 and 4.2, respectively, decrease to 8 and 3.4 at 66 °C. The permselectivity factors $\alpha(CO_2/N_2)$ and $\alpha(CO_2/O_2)$ are independent of p_o in the temperature range 20−70 °C.

In Table 4 the permeability coefficients of several glassy membranes are collected. It can be seen that the permeability coefficients of CO_2, O_2, and N_2 through

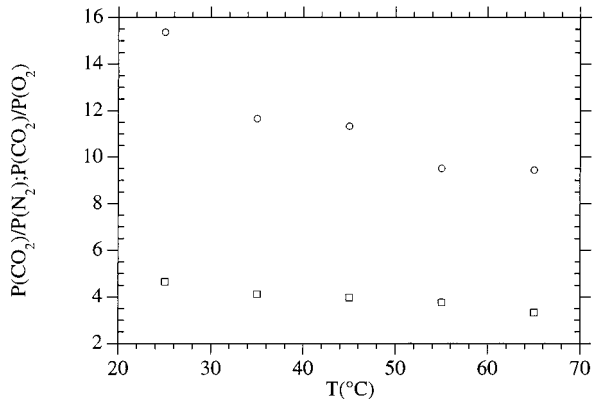

Figure 17. Dependence of the pemselectivity coefficients $\alpha(CO_2/O_2)$ (□) and $\alpha(CO_2/N_2)$ (○) on temperature for $p_o = 15$ cmHg.

Table 4. Permeability Characteristics of Different Membranes[15]

	permeability at 25 °C (in barrers)		
material	O_2	N_2	CO_2
polysulfone	1.1	0.18	6.9
polycarbonate		0.30	8.0
poly(phenylene oxide)		3.81	75.7
LLDPE	4.8	1.5	20

semicrystalline LLDPE membranes are significantly larger than the corresponding values in membranes prepared from polysulfones and polycarbonates. Although glassy membranes prepared from poly(3,4-dimethylphenylene oxide) (PPO) are more permeable to CO_2 and N_2 than the LLDPE membranes, the permselectivity factor $\alpha(CO_2/N_2)$ is near similar in both cases. In general, the value of this factor at 35 °C in the rubbery LLDPE membranes is rather close to that reported for glassy membranes.

It can be concluded from this study that transport of gases through semicrystalline rubbery LLDPE membranes exhibit the same transport pattern that the glassy membranes. The strong dependence of the diffusive characteristics of gases on the pressure difference in the low-pressure region can be interpreted in terms of the dual mode theory. The main difference between the LLDPE membranes used in this study and the glassy membranes lies in the affinity parameter b whose value for CO_2 in the former membranes, is nearly 1 order of magnitude larger than the value of this quantity for the same gas in the latter ones.

References and Notes

(1) *Quality Enhancement and Process Availability in LLDPE Stretch Film by Multisensors and Computerized System*; Forni, C., Coordinator; Brite-Euram-BE Project 4104; Brussels, 1995.
(2) Michaels, A. S.; Bixler, H. *J. Polym. Sci.* **1961**, *50*, 393.
(3) Michaels, A. S.; Bixler, H. *J. Polym. Sci.* **1959**, *41*, 33.
(4) Myers, A. V.; Rogers, C. E.; Stannet, V.; Szwarc, M. *Tappi* **1958**, *41*, 716.
(5) Capaccio, G.; Gibson, A. G.; Ward, I. M. In *Ultrahigh Modulus Polymers*; Ciferri, A., Ward, I. M., Eds.; Applied Science: London, 1979; Chapter I.
(6) Holden, P. S.; Orchard, G. A. J.; Ward, I. M. *J. Polym. Sci., Polym. Phys. Ed.* **1985**, *23*, 709.
(7) Compañ, V.; Andrio, A.; López, M. L.; Riande, E. *Polymer* **1996**, *37*, 5831.
(8) Compañ, V.; Andrio, A.; López, M. L.; Alvarez, C.; Riande, E. *Macromolecules* **1997**, *30*, 3317.
(9) Meares, P. *J. Am. Chem. Soc.* **1954**, *76*, 3415.
(10) Aguilar Vega, M.; Paul, D. A. *J. Polym. Sci, Part B: Polym. Phys.* **1993**, *31*, 1599.
(11) Barrer, R. M. *Trans. Faraday Soc.* **1939**, *35*, 628.
(12) Glatz, F. P.; Mülhaupt, R. *J. Membr. Sci.* **1991**, *90*, 151.
(13) Koros, W. J.; Paul, D. R.; Rocha, A. A. *J. Polym. Sci., Polym. Phys. Ed.* **1976**, *14*, 687.
(14) Frederickson, G. H.; Helfand, E. *Macromolecules* **1985**, *18*, 2201.
(15) Müller-Plathe, F.; Rogers, S. C.; van Gunsteren, W. F. *J. Chem. Phys.* **1993**, *98*, 9895.

MA971600U